Uluslararası İleri Doğa Bilimleri ve Mühendislik Araştırmaları Dergisi
Sayı 8, S. 641-647, 2, 2024

Araştırma Makalesi

IJANSER
https://as-proceeding.com/index.php/ijanser
ISSN: 2980-0811

International Journal of Advanced Natural Sciences and Engineering Researches
Volume 8, pp. 641-647, 2, 2024

Research Article

Asynchronous Machine Controlled by A Series Multi-Cells Converter Using FOPID Controller Tuning with ALO

Mohamed Redha SKENDER [*], Ahmed MEDJBER [2], Fethia HAMIDIA [3], Amel ABBADI [4], Abdelhalim TLEMCANI [5]

[1,2] *Department of Electrical Engineering/ Renewable Energy and Materials Laboratory(REML), Medea University, Algeria*
[3,4,5] *Electrical Engineering/ Laboratory of Electrical Engineering and Automatics (LREA), Medea University, Algeria*

Email of the corresponding author: skender_mohamed@yahoo.fr

(Received: 13 March 2024, Accepted: 14 March 2024)

(4th International Artificial Intelligence and Data Science Congress ICADA 2024, March 14-15, 2024)

ATIF/REFERENCE: Skender, M. R., Medjber, A., Hamidia, F., Abbadi, A. & Tlemcani, A. (2024). Asynchronous Machine Controlled by A Series Multi-Cells Converter Using FOPID Controller Tuning with ALO. *International Journal of Advanced Natural Sciences and Engineering Researches*, 8(2), 641-647.

Abstract **–** This article focuses on a configuration based on multi-cells converters, reducing harmonic distortion. It introduces a fractional-order PID controller optimized by the Antlions optimization algorithm (ALO) for efficient system control in multi-cell converters. The paper's objective is to apply this control scheme to a multi-cell converter connected to an asynchronous machine, offering an effective solution for speed regulation.

Keywords – Nonlinear Control, İnverter, Series Multi-Cells Converter, Fractional Order PID- Antlions Optimization Algorithm, Algorithm, Chopper, Asynchronous Machine.

I. INTRODUCTION

The demand for electrical energy continues to grow, largely fuelled by constant progress in the field of power electronics and advances in semiconductor technology. This development has encouraged the spread of static converters in various sectors, particularly in applications requiring higher power levels. However, the extension to higher voltages inherent in these applications is not without compromises. Increasing the capacity to withstand high voltages leads to a significant deterioration in the static and dynamic properties of the components. As a result, these components offer lower performance than those designed for lower voltages.

In order to solve this problem and exploit higher-performance power electronics components, new converter configurations have emerged, in particular "multilevel converters". Any converter with at least three voltage levels per arm belongs to the family of multilevel converters, indicating that the output voltage can adopt at least three distinct values, as opposed to the two values traditionally used. These systems involve arranging the power switches in series to increase the switched voltage and distribute the voltage stress over different switches. They also allow the use of smaller-calibre components, which are therefore more economical and efficient. The advantage of these multi-level configurations lies in their ability to improve the waveforms and harmonic spectra of the output quantities.

The configuration in this article is based on the use of nested cells (FC - Flying Capacitor topology, or multi-cell topology), which distributes the voltages at the terminals of the semiconductors arranged in series through the interconnection of floating capacitors. This configuration also plays a crucial role in reducing harmonic distortion.

Several control strategies have been suggested for multicell converters, encompassing nonlinear control utilizing input-output linearization [1], robust switching control systems with input delay [2], predictive control [3][4], hybrid control [5][6][7], sliding mode control [8][9][10][11], and exponential mapping function [10]. A summarized fractional-order PID (FOPID) controller was introduced, which includes a λ integral term and a μ derivative term, providing additional degrees of freedom compared to the classical PID controller and making it a popular choice for robust system control [12]. This paper employs the Grey Wolf Optimizer (GWO) algorithm [13] to determine the optimal parameters of the FOPID controller, aiming to minimize the system's performance index. The GWO algorithm is rooted in the hunting approach of the Canadian grey wolf family [13] and has been further developed in [14]. It adjusts the FOPID controller's parameters to meet time and frequency domain specifications, such as settling time, rise time, maximum overshoot, peak time, gain margin, and phase margin.

Asynchronous machines are widely used in applications requiring considerable power. They are characterized by their robustness, durability and ability to offer a wide range of speed variations., It is essential to understand the operating principle of an electric motor to be able to regulate its speed effectively.

This paper's main objective is to apply a fractional-order PID-Grey Wolf optimizer to the multi-levels converter connected to an asynchronous machine. This control scheme is well suited to this type of converter and provides an effective solution for regulating the speed of the asynchronous machine.

II. DC / AC CONVERTER

The DC / AC control stage is ensured by a three-phase multicellular inverter which includes two control loops to improve their efficiency. The inverter regulator includes an internal control loop for DC coupling Voltage (VDC). This voltage control regulates the voltage to its optimum value in order to have the current supplied to the DC link. The second loop is the external control loop for the forward and quadrature currents (Id, Iq) which are supplied by the Phase Locked Loop (PLL). Each of these two loops is controlled by a (FOPID) controller whose gains are modified by applying meta-heuristic techniques (ALO) in order to improve the dynamic performance of the connected PV system to the grid, is to improve the performance of the inverter by modifying the FOPID controllers gains of the current and voltage. For this purpose, there are several meta-heuristic algorithms circulating in the following sections.

Figure 1 shows the scheme of the proposed system [15]. The control of the converter can be done using a PWM technique. To implement the PWM, two superposed triangular carriers are used. Each carrier is connected to one of the two groups of switches controlled complementarily. The positive part of the carrier fixes the switching state of S1, S2 and S3 whereas the negative part controls S'1,S'2 and S'3. Our objective is to regulate the voltages v_{c1} and v_{c2} of the capacitors to their references $\frac{E}{3}$ and $\frac{2E}{3}$ [16].

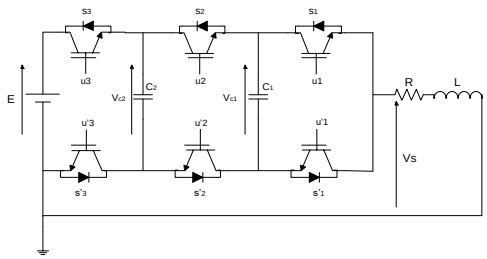

Fig. 1 – Chopper three cells connected to an RL load

The instantaneous state model of a chopper with three cells is expressed as follows:

$$\begin{cases} \dot{x}_1 = f_1(x,u) = \delta_1 c \\ \dot{x}_2 = f_2(x,u) = \delta_2 c \\ \dot{x}_3 = f_3(x,u) = -b \\ y = h(x) = x_3 \end{cases} \quad (1)$$

$(x_1, x_2, x_3)^T = (V_{c1}, V_{c2}, I_{ch})^T$: is the state vector as $x \in \Re^3$

$y = h(x)$: is the measurement vector$y \in \Re$.

(u_1, u_2, u_3) : are controls switches.

$a_1 = a_2 = \frac{1}{C}$, $b_0 = \frac{R}{L}$, $b_1 = \frac{1}{L}$, $\delta_1 = u_2 - u_1$,

$\delta_2 = u_3 - u_2$: are coefficients.

The control scheme for the three- phase inverter is shown in Figure 2.

Figure 3,4 and Figure 5 present the results of simulation for a series multi cells inverter controlled by the PWM technique, the following command sequence is used[15]:

- The voltage source is 1500V, the reference current is 80A.
- The switching frequency $f_{dec} = 20kHz$
- The capacitance of floating sources $C_1 = C_2 = 50\mu F$
- The frequency of the modulant $f_{mod} = 500Hz$

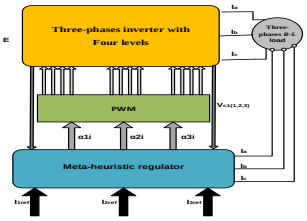

Fig. 2 – Structure FOPID-ALO control inverter

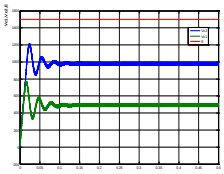

Fig. 3 – Voltage evolutions V_{C1} ,V_{C2} at the capacitors C1 and C2 terminals.

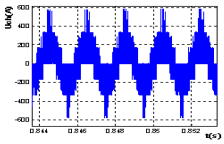

Fig. 4 – the voltage curve U_{ch} at the terminals of the inverter output)

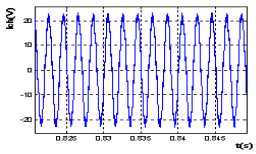

Fig. 5 – the current curve I_{ch} at the terminals of the inverter output).

Our objective is to regulate the voltages v_{c1} and v_{c2} of capacitors to their references $\frac{E}{3} = \frac{1500}{3} = 500\text{V}$ and $\frac{2E}{3} = \frac{2\times1500}{3} = 1000V$ as shown in Figure 3 and the load current must reach its reference value $I_{ref} = 80A$ as shown in Figure 5 .

III. FRACTIONAL-ORDER PID CONTROLLER.

The FOPID controller control loop feedback mechanism and reduce the error between a measured variable and the desired set point of a process. The generalized transfer function is given by

$$C(s) = \frac{U(s)}{E(s)} = K_P + \frac{K_I}{s^\lambda} K_D s^\mu \quad (\lambda, \mu \geq 0) \quad (2)$$

where $C(s)$represents the controller output; $U(s)$ and $E(s)$ are the control signal and the error signal, respectively; The FOPID equation has five unknown parameters, KP, KI, and Kd are the proportional, integral, and derivative constant gains, respectively; λ is the order of integration; and μ is the order of differentiator .If λ = 1 and μ = 1, a classical PID controller is recovered[17].

The block diagram of control system employing Soft computing FOPID control action is shown in Fig.6.

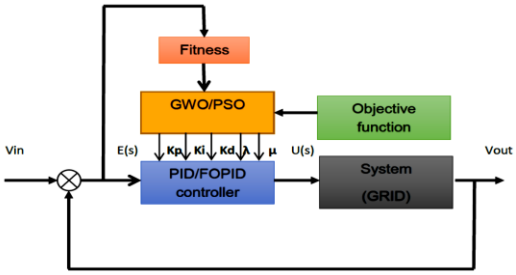

where
$Vin(s)$: Input Signal
$E(s)$: Error Signal
Vout(s):Output Signal
$U(s)$:Control Signal

Fig. 6 – A block diagram of Intelligent FOPID controller

- *cost function*

To evaluate the qualities of the regulator, there are different types of control such as the Integral of Squared Error (ISE), Integral of Absolute Error (IAE), Integral of Time Squared Error (ITSE) , and Integral of Time Absolute Error (ITAE)[18] ..

A drawback of the IAE and ISE categories which influence all errors equally and independent of time) is that they may train in a response with a long settling time and relatively small overshoot [18]. To surmount this disadvantage, an ITAE is used as fitness function.

Therefore, the controller can be evaluated using the following performance index:

$$j(K_p, K_i, K_d, \mu, \lambda) = \int_0^\infty t|e(t)|dt \quad (3)$$

j is called as ITAE. It means that the controlled object is close to the set point model. Where t is the time and $e(t)$ is the error between reference and controlled variable.

IV. ANTLIONS OPTIMIZATION ALGORITHM (ALO)

ALO is a stochastic algorithm that was enthused from the antlions hunting behavior (Mirjalili, 2015a). According to Fig. 5, the ants that represent the preys moves randomly over research space using Eq. (10) (Mirjalili, 2015a). The ants random walks are affected by antlions' traps as in Eqs. (11) and (12) (Mirjalili, 2015a). Depending on the fitness function, the ALO uses roulette wheel to allow the antlion to catch their prey (Dubey et al., 2016; Mirjalili, 2015a; Saxena and Kothari, 2016). One the ants attain the bottom of the pit, their positions are the best positions that correspond to antlions positions as in Eq. (13). The up- dating antlions positions is performed to run the process until the ter- mination criterion is satisfied(Mirjalili, 2015a; Mirjalili et al., 2016; Saxena and Kothari, 2016).

$$X_i^t = \frac{(X_i^t - a) * (d_i - c_i^t)}{(d_i^t - a_i)} + c_i$$

$$c_i^t = Antlion_i^t + c^t$$

$$d_i^t = Antlion_i^t + d^t$$

$$Antlion_i^t = Ant_i^t \, iff \, (Ant_i^t) > f\,(Antlion_i^t)$$

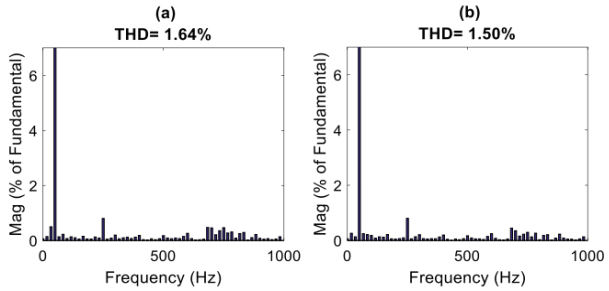

- Encircling: The modeling of The encirclement of

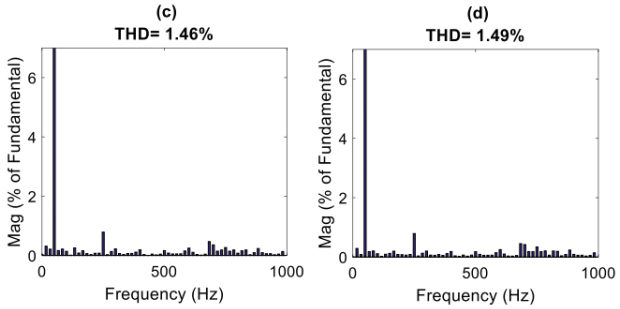

Fig. 6 – FFT analysis of PV grid current

Detailed flowchart of the GWO algorithm is shown in Fig. 7.

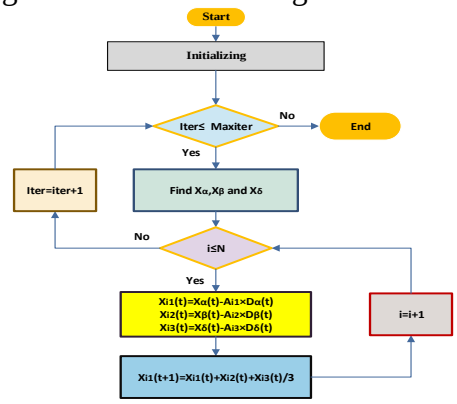

Fig. 7 – The flowchart of the ALO algorithm

Although ALO is simple and applicable for several applications, it suffers from lack of population diversity, the imbalance between the exploitation and exploration, and the premature convergence[19][20][21][22].

V. RESULTS

In this simulation we will see the different results when the inverter is loaded with an asynchronous machine. We will use PWM control and FOPID-ALO control.

No-load starting with the introduction of an asynchronous motor load torque, by applying a load torque of l5 N.m at time t = 1 s, the following figures show the results obtained according .

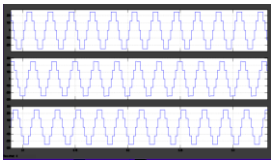

Fig. 8 –inverter composite voltages (PWM control)

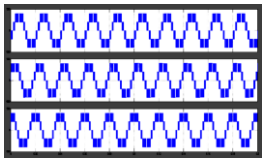

Fig. 9 – inverter composite voltages (FOPID-ALO control)

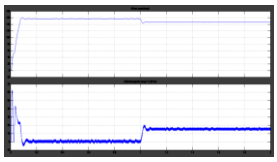

Fig. 10 – motor speed and electromagnetic torque(PWM control)

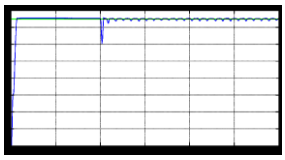

Fig. 11 – motor speed(FOPID-ALO control)

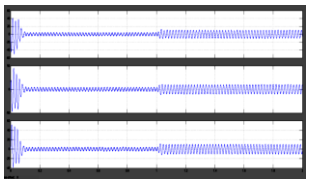

Fig. 12 – asynchronous motor currents under load(PWM control)

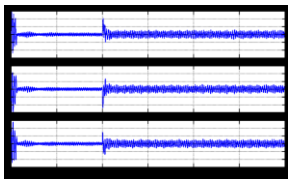

Fig. 13 – asynchronous motor currents under load(FOPID-ALO control)

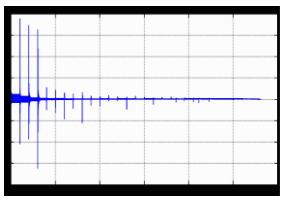

Fig. 14 – motor electromagnetic torque(PWM control)

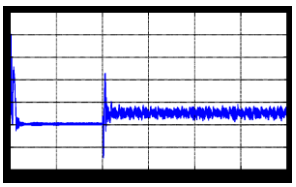

Fig. 15 – motor electromagnetic torque(FOPID-ALO control)

VI. DISCUSSION

In figure 10, at start-up, the speed is slightly higher than the reference, and when the load torque is introduced at t=1s, we see a disturbance rejection that exceeds the acceptable error.

When the FOPID-ALO In figure 11 is applied, the speed is lower than the reference, and the disturbance rejection can be seen at the moment the load torque is applied.

VII. CONCLUSION

This paper's main objective is to apply a fractional-order PID- Antlions optimization algorithm to the multi-levels converter connected to an asynchronous machine. This control scheme is well suited to this type of converter and provides an effective solution for regulating the speed of the asynchronous machine.

REFERENCES

[1] G. Gateau, M. Fadel, P. Maussion, R. Bensaid, and T. A. Meynard, *Multicell converters: Active control and observation of flying-capacitor voltages*, IEEE Trans. Ind. Electron., vol. 49, no. 5, pp. 998–1008, Oct. 2002.

[2] V. Filipovic, *Robust switching control systems with input delay*, Stud. Informatics Control, vol. 20, no. 4, pp. 411–420,

2011.
[3] F. Defaÿ, A. M. Llor, and M. Fadel, *A predictive control with flying capacitor balancing of a multicell active power filter*, IEEE Trans. Ind. Electron., vol. 55, no. 9, pp. 3212–3220, 2008.
[4] P. Lezana, R. Aguilera, and D. E. Quevedo, *Model predictive control of an asymmetric flying capacitor converter*, IEEE Trans. Ind. Electron., vol. 56, no. 6, pp. 1839–1846, 2009.
[5] M. R. Skender and A. Tlemcani, *Application on the series multi-cells converter for implementation and comparison between a higher order sliding mode control and simple order*, J. Electr. Electron. Eng., vol. 8, no. 1, pp. 31–36, 2015.
[6] M. R. Skender and A. Tlemcani, *Sliding mode observer control founded to series multi-cell converter*, 2015 4th Int. Conf. Electr. Eng. ICEE 2015, pp. 1–5, Feb. 2015.
[7] M. Bâja, D. Patino, H. Cormerais, P. Riedinger, and J. Buisson, *Hybrid control of a three-level three-cell dc-dc converter*, Proc. Am. Control Conf., pp. 5458–5463, 2007.
[8] M. R. Skender and A. Tlemcani, *Sliding mode observer control founded to series multi-cell converter* | IEEE Conference Publication | IEEE Xplore, IEEE Xplore, Feb. 25, 2016. https://ieeexplore.ieee.org/document/7416842 (accessed Dec. 23, 2021).
[9] L. Amet, M. Ghanes, and J. P. Barbot, *Direct control based on sliding mode techniques for multicell serial chopper*, Proc. Am. Control Conf., pp. 751–756, 2011.
[10] M. Djemai, K. Busawon, K. Benmansour, and A. Marouf, *High-order sliding mode control of a DC motor drive via a switched controlled multi-cellular converter*, https://doi.org/10.1080/00207721.2010.545492, vol. 42, no. 11, pp. 1869–1882, Nov. 2011.
[11] S. Meradi, K. Benmansour, K. Herizi, M. Tadjine, and M. S. Boucherit, *Sliding mode and fault tolerant control for multicell converter four quadrants*, Electr. Power Syst. Res., vol. 95, pp. 128–139, Feb. 2013.
[12] P. I., *Fractional-order systems and fractional-order controllers*, Slovak Acad. Sci., vol. 12, no. 3, pp. 1–18, 1994.
[13] C. Muro, R. Escobedo, L. Spector, and R. P. Coppinger, *Wolf-pack (Canis lupus) hunting strategies emerge from simple rules in computational simulations*, Behav. Processes, vol. 88, no. 3, pp. 192–197, Nov. 2011.
[14] S. D, *Empowerment as a New Approach in the Management*, Int. J. Account. Bus. Manag., vol. 4, no. 2, pp. 209–221, 2015.
[15] M. R. Skender, A. Tlemçani, and H. Nouri, *A novel observer algorithm of voltages across capacitors based on the higher sliding mode control: Application to multi-cells converter*, Int. J. Model. Identif. Control, vol. 27, no. 2, pp. 136–145, 2017.
[16] A. E. W. H. Kahlane, L. Hassaine, and M. Kherchi, *LCL filter design for photovoltaic grid connected systems*, Third Int. Semin. new Renew. energies, vol. 8, no. 2, pp. 227–232, 2014.
[17] A. Naserbegi, M. Aghaie, and A. Zolfaghari, *Implementation of Grey Wolf Optimization (GWO) algorithm to multi-objective loading pattern optimization of a PWR reactor*, Ann. Nucl. Energy, vol. 148, p. 107703, 2020.
[18] E. Emary, H. M. Zawbaa, and C. Grosan, *Experienced Gray Wolf Optimization Through Reinforcement Learning and Neural Networks*, IEEE Trans. Neural Networks Learn. Syst., vol. 29, no. 3, pp. 681–694, 2018.
[19] A. A. Heidari and P. Pahlavani, *An efficient modified grey wolf optimizer with Lévy flight for optimization tasks*, Appl. Soft Comput., vol. 60, pp. 115–134, Nov. 2017.
[20] W. Long, J. Jiao, X. Liang, and M. Tang, *An exploration-enhanced grey wolf optimizer to solve high-dimensional numerical optimization*, Eng. Appl. Artif. Intell., vol. 68, pp. 63–80, Feb. 2018.
[21] C. Lu, L. Gao, and J. Yi, *Grey wolf optimizer with cellular topological structure*, Expert Syst. Appl., vol. 107, pp. 89–114, Oct. 2018.
[22] Q. Tu, X. Chen, and X. Liu, *Hierarchy Strengthened Grey Wolf Optimizer for Numerical Optimization and Feature Selection*, IEEE Access, vol. 7, pp. 78012–78028, 2019.
[23] M. Hlaili and H. Mechergui, *Comparison of Different MPPT Algorithms with a Proposed One Using a Power Estimator for Grid Connected PV Systems*, Int. J. Photoenergy, vol. 2016, 2016.